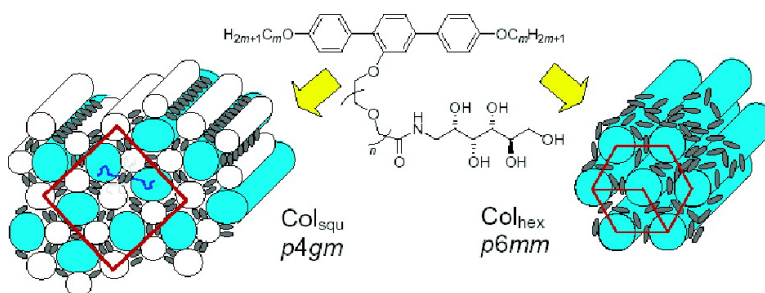


Carbohydrate Rod Conjugates: Ternary Rod–Coil Molecules Forming Complex Liquid Crystal Structures

Bin Chen, Ute Baumeister, Gerhard Pelzl, Malay Kumar Das, Xiangbing Zeng, Goran Ungar, and Carsten Tschierske

J. Am. Chem. Soc., **2005**, 127 (47), 16578-16591 • DOI: 10.1021/ja0535357 • Publication Date (Web): 02 November 2005

Downloaded from <http://pubs.acs.org> on March 25, 2009



More About This Article

Additional resources and features associated with this article are available within the HTML version:

- Supporting Information
- Links to the 24 articles that cite this article, as of the time of this article download
- Access to high resolution figures
- Links to articles and content related to this article
- Copyright permission to reproduce figures and/or text from this article

[View the Full Text HTML](#)



Carbohydrate Rod Conjugates: Ternary Rod–Coil Molecules Forming Complex Liquid Crystal Structures

Bin Chen,[†] Ute Baumeister,[‡] Gerhard Pelzl,[‡] Malay Kumar Das,[‡] Xiangbing Zeng,[§] Goran Ungar,[§] and Carsten Tschierske^{*†}

Contribution from the Institute of Organic Chemistry, University Halle, Kurt-Mothes-Strasse 2, D-06120 Halle, Germany, Institute of Physical Chemistry, University Halle, Mühlpforte 1, D-06108 Halle, Germany, and Centre for Molecular Materials, University of Sheffield, Robert Hadfield Building Mappin Street, Sheffield S1 3JD, Great Britain

Received May 31, 2005; Revised Manuscript Received September 14, 2005; E-mail: carsten.tschierske@chemie.uni-halle.de

Abstract: T-shaped polyphilic triblock molecules, consisting of a rodlike *p*-terphenyl unit, a hydrophilic and flexible laterally attached oligo(oxyethylene) chain terminated by an 1-acylamino-1-deoxy-D-sorbitol unit, and two end-attached lipophilic alkyl chains, have been synthesized by palladium-catalyzed cross-coupling reactions as the key steps. The thermotropic liquid crystalline behavior of these compounds was investigated by polarized light microscopy, differential scanning calorimetry (DSC), and X-ray scattering. We investigated the mode of self-organization as a function of the length and position of the lateral polar chain and the length of the terminal alkyl chains. Depending on the size of the polar and lipophilic segments, a series of unusual liquid crystalline phases was detected. In three of these phases, the space is divided into three distinct periodic subspaces. In addition to a hexagonal channeled layer phase (ChL_{hex}) consisting of layers that are penetrated by polar columns, there are also two honeycomb-like network structures formed by square (Col_{squ}/p4mm) or pentagonal cylinders (Col_{squ}/p4gm). The cylinder walls consist of the terphenyl units fused by columns of alkyl chains, and the interior contains the polar side chains. In addition, a hexagonal columnar phase was observed in which the polar columns are organized in a continuum of terphenyls and alkyl chains with an organization of the terphenyl cores tangentially around the columns with the long axis perpendicular to the columns. For one compound, a reversal of birefringence was observed, which is explained by a reorientation of the terphenyl cores. The addition of protic solvents induces lamellar phases.

Introduction

The optimization of materials properties requires control of the organization of molecules.¹ The design of solid crystals with a predetermined structure, for example, is still more a hit-or-miss activity rather than a rational design.^{2,3} The difficulty lies in the large number of intermolecular interactions with similar energies that are hard to predict and evaluate accurately. In contrast, in fluid systems some of the interactions are averaged out by molecular motion, leaving only the strongest determining the overall structure and simplifying the problem considerably. Liquid crystals⁴ are ordered fluids in which the segregation of incompatible units⁵ and parallel alignment of rigid units combine

to give rise to positional and orientational long-range order. Increasing the complexity of liquid crystals^{6–8} should open new perspectives for their use as sophisticated functional materials.⁹ Furthermore, it is hoped that such systems might contribute to the fundamental understanding of self-assembly in other complex systems, such as solid crystals and living systems.

On the basis of the concept of competitive polyphilicity, the bolaamphiphiles shown in Figure 1, incorporating a rigid biphenyl core, a pair of 2,3-dihydroxypropoxy terminal groups,

[†] Institute of Organic Chemistry.

[‡] Institute of Physical Chemistry.

[§] University of Sheffield.

- (1) (a) Petty, M. C.; Bryce, M. R.; Bloor, D. *Introduction to Molecular Electronics*; Edward Arnold: London, 1995. (b) Simon, J.; Bassoul, P. *Design of Molecular Materials: Supramolecular Engineering*; John Wiley: Chichester, U.K., 2000.
- (2) Lee, S.; Mallik, A. B.; Xu, Z.; Lobkowsky, E. B.; Tran, L. *Acc. Chem. Res.* **2005**, *38*, 251–261.
- (3) Recent reviews about crystal engineering: (a) Braga, D. *Chem. Commun.* **2003**, 2751–2754. (b) Brammer, L. *Chem. Soc. Rev.* **2004**, *33*, 476–489. (c) Zaworotko, M. J. *Chem. Commun.* **2001**, 1–9. (d) Sarma, J. A. R. P.; Desiraju, G. R. *Cryst. Growth Des.* **2002**, *2*, 93–100. (e) Sharma, C. V. K. *Cryst. Growth Des.* **2002**, *2*, 565–474. (f) Robson, R. *J. Chem. Soc., Dalton Trans.* **2000**, 3735–3744.
- (4) Demus, D.; Goodby, J.; Gray, G. W.; Spiess, H. W.; Vill, V. *Handbook of Liquid Crystals*; Wiley-VCH: Weinheim, Germany, 1998.

- (5) (a) Tschierske, C. *J. Mater. Chem.* **1998**, *8*, 1485–1508. (b) Chen, W.; Wunderlich, B. *Macromol. Chem. Phys.* **1999**, *200*, 283–311. (c) Tschierske, C. *J. Mater. Chem.* **2001**, *11*, 2647–2671.
- (6) (a) Goodby, J. W.; Mehl, G. H.; Saez, I. M.; Tuffin, R. P.; Mackenzie, G.; Auzély-Velty, R.; Benvegnu, T.; Plusquellec, D. *Chem. Commun.* **1998**, 2057–2070. (b) Tschierske, C. *Ann. Rep. Prog. Chem., Ser. C* **2001**, *97*, 191–267. (c) Tschierske, C. *Curr. Opin. Colloid Interface Sci.* **2002**, *7*, 69–80.
- (7) (a) Barberá, J.; Donnio, B.; Giménez, R.; Guillon, D.; Marcos, M.; Omenat, A.; Serrano, J. L. *J. Mater. Chem.* **2001**, *11*, 2808–2813. (b) Ungar, G.; Liu, Y.-S.; Zeng, X.-B.; Percec, V.; Cho, W.-D. *Science* **2003**, *299*, 1208–1211. (c) Zeng, X.-B.; Ungar, G.; Liu, Y.-S.; Percec, V.; Dulcey, A. E.; Hobs, J. *Nature* **2004**, *428*, 157–160. (d) Percec, V.; Mitchell, C. M.; Cho, W.-D.; Uchida, S.; Glodde, M.; Ungar, G.; Zeng, X.; Liu, Y.; Balagurusamy, V. S. K.; Heiney, P. A. *J. Am. Chem. Soc.* **2004**, *126*, 6078–6094. (e) Gehring, L.; Bourgogne, C.; Guillon, D.; Donnio, B. *J. Am. Chem. Soc.* **2004**, *126*, 3856–3867.
- (8) (a) Lee, M.; Cho, B.-K.; Zin, W.-C. *Chem. Rev.* **2001**, *101*, 3869–3892. (b) Jin, L. Y.; Bae, J.; Ahn, J.-H.; Lee, M. *Chem. Commun.* **2005**, 1197–1199. (c) Kim, J.-K.; Hong, M.-K.; Ahn, J.-H.; Lee, M. S. *Angew. Chem., Int. Ed.* **2005**, *44*, 328–332.
- (9) Kato, T. *Science* **2002**, *295*, 2414–2418.

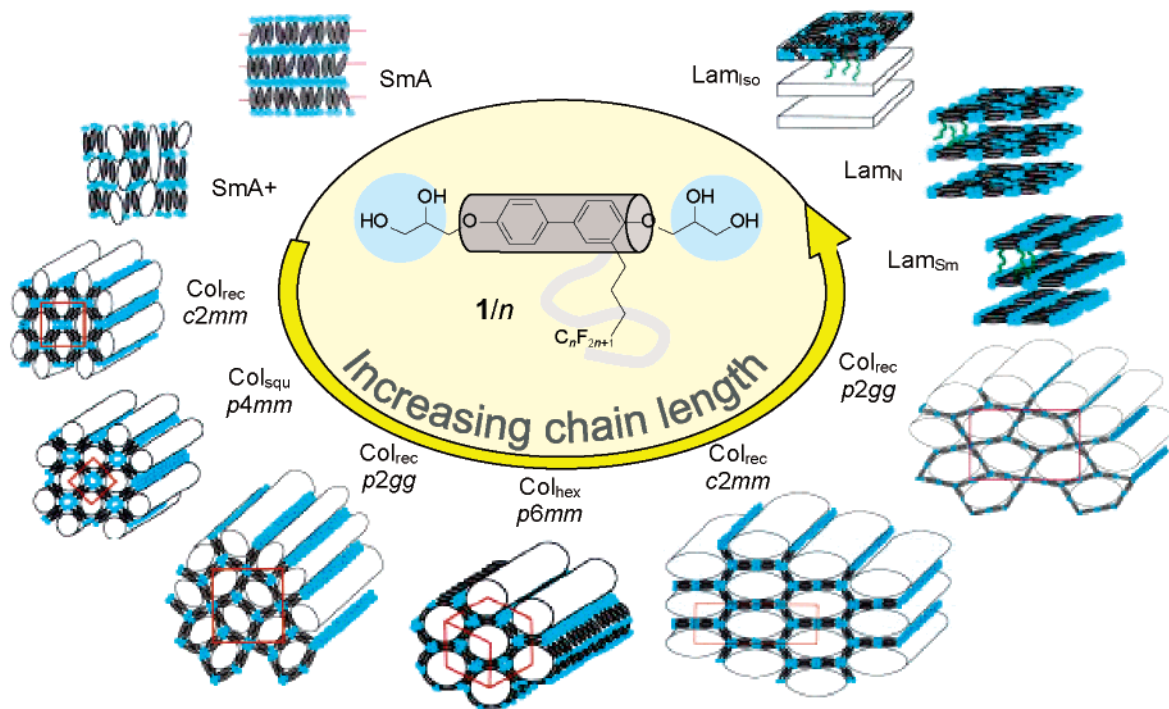


Figure 1. Mesophases reported for calamitic bolaamphiphiles with nonpolar lateral chains,^{10,a,b} abbreviations of the mesophase types: SmA = smectic A phase (molecules are organized in layers without in-plane order and in average perpendicular to the layers). Col_{rec} = rectangular columnar phase. Col_{squ} = square columnar phase. Col_{hex} = hexagonal columnar phase. Lam = laminated phase; the Lam_{iso} phase is built up by a sequence of two sets of isotropic sublayers; in the Lam_N phase the rodlike units have an orientational order, and these units are arranged in average parallel to the layers; in the Lam_{Sm} phase the molecules are thought to adopt an additional positional order within the layers.

and a lipophilic lateral chain, have been developed recently.^{10,11} For these compounds, a series of new and complex types of organizations in liquid crystal (LC) systems has been discovered. As shown in Figure 1, different honeycomb-like cylinder structures¹⁰ and lamellar phases¹¹ were detected.

In this report, another class of ternary block molecules is described in which the position of amphiphilic groups is reversed; that is, the polar group is attached to a lateral position on the rigid core (1,1'-4'1''-terphenyl units in all cases), and the lipophilic chains are tethered at the termini. Previously, we have sporadically reported selected examples of such facial amphiphiles with the lateral chains ending with different polar groups, mainly carboxylate,¹² COOH groups,¹³ or diol¹⁴ groups. Herein, the development of soft-matter nanostructures is reported for several complete series of facial amphiphiles with a bulky carbohydrate unit as the polar group (1-acylamino-1-deoxy-D-sorbitol derivatives).^{15,16} A series of seven different liquid

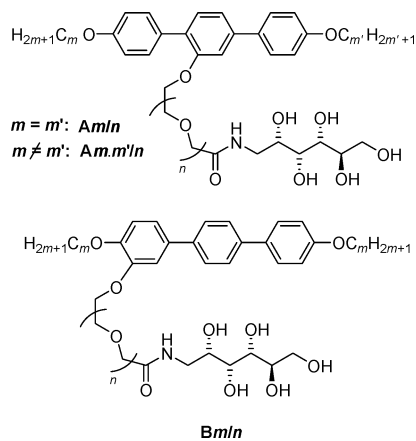
crystalline phases in total are found. The evolution of mesophase structures is monitored in a systematic way as a function of length of the terminal alkyl chains and as a function of the number of oxyethylene units in the polar chains. In addition, the effects of the position of the polar group, of branching of the alkyl chains, and of the nonsymmetric distribution of these chains at both ends are reported. The results provide a lesson in principles of molecular self-assembly in soft matter and offer clues for designing molecules and tailoring complex superstructures in a predictable way. Although there are some similarities with the phase sequence observed for the bolaamphiphiles, there are also significant differences due to the exchange of positions of the amphiphilic groups. In particular, a new hexagonal columnar mesophase is reported here for the first time. Its polar columns penetrate an orientationally ordered continuum, and it shows a temperature-induced reversal of mesogen alignment with respect to the column axis. Furthermore, it is shown that lamellar phases are induced by protic solvents, indicating amphotropic¹⁷ behavior of these compounds.

The general structure of the compounds investigated is shown below. The polar hydrogen-bonding units are attached via an amide group and flexible oligo(oxyethylene) chains of variable length ($n = 0-6$) to the rigid and linear *p*-terphenyl core either

- (10) (a) Kölbl, M.; Beyersdorff, T.; Cheng, X.-H.; Tschierske, C. *J. Am. Chem. Soc.* **2001**, *123*, 6809–6818. (b) Cheng, X.-H.; Prehm, M.; Das, M. K.; Kain, J.; Baumeister, U.; Diele, S.; Leine, D.; Blume, A.; Tschierske, C. *J. Am. Chem. Soc.* **2003**, *125*, 10977–10996. (c) Cheng, X.-H.; Das, M. K.; Baumeister, U.; Diele, S.; Tschierske, C. *J. Am. Chem. Soc.* **2004**, *126*, 12930–12940.
- (11) (a) Prehm, M.; Cheng, X.-H.; Diele, S.; Das, M. K.; Tschierske, C. *J. Am. Chem. Soc.* **2002**, *124*, 12072–12073. (b) Cheng, X.-H.; Das, M. K.; Diele, S.; Tschierske, C. *Angew. Chem., Int. Ed.* **2002**, *41*, 4031–4035. (c) Prehm, M.; Diele, S.; Das, M. K.; Tschierske, C. *J. Am. Chem. Soc.* **2003**, *125*, 614–615. (d) Patel, N. M.; Dodge, M. R.; Zhu, M.-H.; Petschek, R. G.; Rosenblatt, C.; Prehm, M.; Tschierske, C. *Phys. Rev. Lett.* **2004**, *92*, 015501. (e) Patel, N. M.; Syed, I. M.; Rosenblatt, C.; Prehm, M.; Tschierske, C. *Liq. Cryst.* **2005**, *32*, 55–61.
- (12) Chen, B.; Zeng, X.-B.; Baumeister, U.; Diele, S.; Ungar, G.; Tschierske, C. *Angew. Chem., Int. Ed.* **2004**, *43*, 4621–4625.
- (13) Chen, B.; Zeng, X.-B.; Baumeister, U.; Ungar, G.; Tschierske, C. *Science* **2005**, *307*, 96–99.
- (14) (a) Schröter, J. A.; Plehnert, R.; Tschierske, C.; Katholy, S.; Janietz, D.; Penacorada, F.; Brehmer, L. *Langmuir* **1997**, *13*, 796–800. (b) Plehnert, R.; Schröter, J. A.; Tschierske, C. *Langmuir* **1999**, *15*, 3773–3781.

- (15) Preliminary communication: Chen, B.; Baumeister, U.; Diele, S.; Das, M. K.; Zeng, X.-B.; Ungar, G.; Tschierske, C. *J. Am. Chem. Soc.* **2004**, *126*, 8608–8609.
- (16) Carbohydrate LC incorporating terminally attached rodlike segments: (a) Müller, H.; Tschierske, C. *Chem. Commun.* **1995**, 645–646. (b) Ewing, D. F.; Glew, M.; Goodby, J. W.; Haley, J. A.; Kelly, S. M.; Komanschek, B. U.; Letellier, P.; Mackenzie, G.; Mehl, G. *J. Mater. Chem.* **1998**, *8*, 871–880. (c) Lafont, N. L. D.; Dumoulin, F.; Boullanger, P.; Mackenzie, G.; Kouwer, P. H. J.; Goodby, J. W. *J. Am. Chem. Soc.* **2003**, *125*, 15499–15506.
- (17) Reviews about amphotropic LC: (a) Tschierske, C. *Prog. Polym. Sci.* **1996**, *21*, 775–852. (b) Tschierske, C. *Curr. Opin. Colloid Interface Sci.* **2002**, *7*, 355–370.

in a central position (compounds **Am/n**, where *m* is the length of the terminal alkyl chains and *n* is the number of oxyethylene units in the lateral chain) or in a peripheral position (compounds **Bm/n**).¹⁸ The flexible polyether chain has two functions: it increases the size of the lateral group and decouples the carbohydrate unit from the rigid core, thus reducing the melting point and broadening the LC range. The terminal chains are linear alkyls with identical length at both ends (*m* = 4–16) in most cases. In selected examples, the terminal chains are (racemic) branched 3,7-dimethyloctyl groups (**A10*/3** and **A10*/4**), whereas in others, the chains at each end have very different lengths (hexyl and hexadecyl).

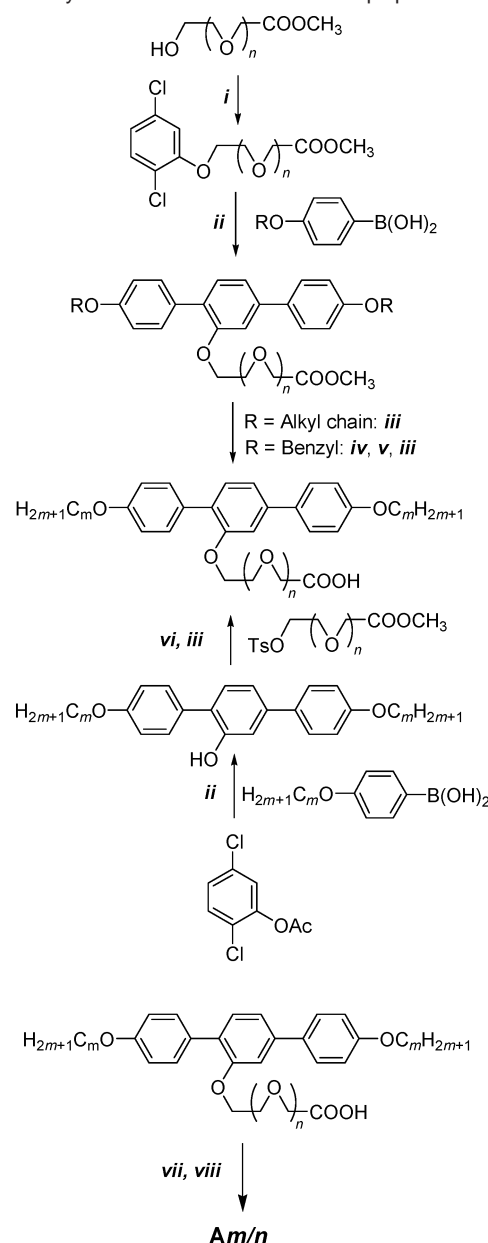


Results and Discussion

1. Synthesis. Three different strategies were used to synthesize compounds **Am/n** containing two identical alkyl chains and the lateral polar chain in the central 2'-position. The routes to the carboxylic acids are outlined in Scheme 1 (see also Schemes S1 and S2 in the Supporting Information). In all synthetic routes, the key step is a Suzuki-type coupling¹⁹ of a 2-substituted 1,4-dichlorobenzene derivative with two equiv of a 4-substituted benzenboronic acid using Pd(OAc)₂, 2-(di-*tert*-butylphosphino)biphenyl as a catalyst and KF as the base (Buchwald procedure).²⁰ The amides **Am/n** were prepared from these acids by esterification with pentafluorophenol using DCC as a condensing agent followed by aminolysis of the resulting pentafluorophenyl esters²¹ with 1-amino-1-deoxy-D-sorbitol. The 2-substituted compounds **Bm/n** and the compounds **Am.m'/n** with two different alkyl chains at the terphenyl core were built up in a stepwise manner as shown in Schemes S3–S5 of the Supporting Information. All final products were purified by column chromatography on silica gel, then by repeated crystallization from appropriate solvents and characterized by ¹H, ¹³C NMR, and elemental analysis. The purity was additionally checked by TLC. The experimental details and analytical data of all compounds are collated in the SI.

2. Mesomorphic Properties. The synthesized compounds were investigated by polarized light microscopy, differential scanning calorimetry (DSC), and X-ray scattering.²² Selected

Scheme 1. Synthetic Route to the Facial Amphiphiles **Am/n**^a



^a Reagents and conditions: *i*) 1. TsCl, Py, 0 °C; 2. 2,5-dichlorophenol, K₂CO₃, CH₃CN, (n-Bu)₄NI, reflux, 8 h; *ii*) Pd(OAc)₂, 2-(di-*tert*-butylphosphino)biphenyl, KF, THF, rt, 24 h; *iii*) NaOH, H₂O, reflux 16 h, then HCl (10% aq), Et₂O, rt, 1 h; 16 h; *iv*) Pd(OH)₂, MeOH, cyclohexene, reflux; *v*) C_mH_{2m+1}Br, K₂CO₃, CH₃CN, (n-Bu)₄NI, reflux, 8 h; *vi*) K₂CO₃, CH₃CN, (n-Bu)₄NI, reflux, 8 h; *vii*) pentafluorophenol, DCC, THF, 20 °C, 24 h; *viii*) 1-amino-1-deoxy-D-sorbitol, THF, 24 h.

compounds were investigated using synchrotron radiation, and the precise diffraction data obtained in this way were used to calculate electron density maps²³ that additionally confirmed the predicted mesophase structures. The transition temperatures and corresponding enthalpy values are collected in Tables 1–3.

(18) Rod-coil molecules with a terminally attached carbohydrate unit: Kim, B.-S.; Yang, W.-Y.; Ryu, J.-H.; Yoo, Y.-S.; Lee, M. *Chem. Commun.* **2005**, 2035–2037.

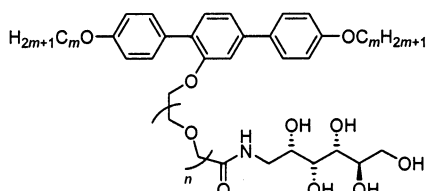
(19) Miyaura, N.; Suzuki, A. *Chem. Rev.* **1995**, *95*, 2457–2483.

(20) Wolfe, J. P.; Singer, R. A.; Yang, B. H.; Buchwald, S. L. *J. Am. Chem. Soc.* **1999**, *121*, 9550–9561.

(21) Baars, M. W. P. L.; Söntjens, S. H. M.; Fischer, H. M.; Peerlings, H. W. I.; Meijer, E. W. *Chem.-Eur. J.*, **1998**, *4*, 2456–2466.

(22) Most of the compounds are hygroscopic. To remove traces of water, the open samples were heated to 170 °C for ca. 5 s; then, they were immediately covered or sealed and investigated. The weight loss corresponds to the amount of water absorbed by the material, which can be determined according to: Dunkel, R.; Hahn, M.; Borisch, K.; Neumann, B.; Rüttinger, H.-H.; Tschierske, C. *Liq. Cryst.* **1998**, *24*, 211–213. Filling of the capillaries for X-ray investigations was also done at that temperature.

(23) (a) Balagurusamy, V. S. K.; Ungar, G.; Percec, V.; Johansson, G. *J. Am. Chem. Soc.* **1997**, *119*, 1539–1555. (b) Dukeson, D. R.; Ungar, G.; Balagurusamy, V. S. K.; Percec, V.; Johansson, G.; Glodde, M. *J. Am. Chem. Soc.* **2003**, *125*, 15974–15980.

Table 1. Mesophases, Phase Transition Temperatures, Phase Transition Enthalpy Values, and Other Parameters of the Facial Amphiphiles **A_m/n^a**


compd	<i>m</i>	<i>n</i>	<i>T</i> /°C			lattice parameter (nm) (<i>T</i> /°C) ^c	<i>V</i> _{cell} ^d (nm ³)	<i>V</i> _{mol} ^e (nm ³)	<i>n</i> _{cell} ^f (<i>n</i> _{cy})			
			<i>ΔH</i> /kJ·mol ^{-1b}									
A4/2	4	2	Cr 86	Col _{squ} /p4gm	102	Col _{hex}	112	<i>I</i>	<i>a</i> _{hex} = 3.7 (105) <i>a</i> _{squ} = 7.1 (90)	5.3 22.7	0.92	5.8 24.7 (6.2)
A4/3	4	3	Cr 70	Col _{hex}	102	<i>I</i>			<i>a</i> _{hex} = 4.0 (90) <i>a</i> _{hex} = 4.2 (50)	6.2 6.9	0.98	6.3 7.0
A4/4	4	4	Cr 56	Col _{hex}	97	<i>I</i>			<i>a</i> _{hex} = 4.2 (85) <i>a</i> _{hex} = 4.4 (55)	6.9 7.5	1.04	6.6 7.2
A6/3	6	3	Cr 53	Col _{squ} /p4gm+	118	<i>I</i>			<i>a</i> _{squ1} = 7.9 (100) ^g <i>a</i> _{squ2} = 3.6 (100) ^g	28.1 5.8	1.08	26.0 (6.5) 5.4
A6/4 ¹³	6	4	Cr 47	Col _{squ} /p4gm	104	Col _{hex}	111	<i>I</i>	<i>a</i> _{squ} = 8.0 (98) <i>a</i> _{hex} = 4.3 (108)	28.8 7.2	1.14	25.3 (6.3) 6.3
A6/5	6	5	Cr 51	Col _{squ} /p4gm	79	Col _{hex}	108	<i>I</i>	<i>a</i> _{squ} = 8.3 (70) <i>a</i> _{hex} = 4.7 (80)	31.0 8.6	1.19	26.1 (6.5) 7.2
A6/6	6	6	G -6	Col _{hex}	102	Iso			<i>a</i> _{hex} = 4.9 (80)	9.4	1.25	7.5
A8/3	8	3	G 2	Col _{squ} /p4mm	145	<i>I</i>			<i>a</i> _{squ} = 3.7 (140) <i>a</i> _{squ} = 4.0 (25)	6.2 7.2	1.18	5.3 6.1
A10/0 ^{h,26}	10	0	Cr 112	SmA	147	<i>I</i>			<i>d</i> = 3.3 (120)			
A10/1	10	1	G 14	ChL _{hex}	147	<i>I</i>			<i>a</i> = 4.0, <i>c</i> = 3.8 (100)	52.7	1.16	45
A10/2	10	2	Cr 38	ChL _{hex}	107	Col _{squ} /p4mm	143	<i>I</i>	<i>a</i> _{squ} = 3.7 (130) <i>a</i> = 4.4, <i>c</i> = 3.8 (90) ⁱ	6.2 63.7	1.22	5.1 52
A10/3 ¹⁵	10	3	G 2	Col _{squ} /p4mm	144	<i>I</i>			<i>a</i> _{squ} = 3.9 (130)	6.8	1.28	5.3
A10/4 ¹⁵	10	4	G -5	Col _{squ} /p4mm	141	<i>I</i>			<i>a</i> _{squ} = 4.0 (135)	7.2	1.33	5.4
A10/6 ¹⁵	10	6	G -12	Col _{squ} /p4mm	117	<i>I</i>			<i>a</i> _{squ} = 4.2 (90)	7.9	1.45	5.4
A10*/3	10* ^j	3	G -2	Col _{squ} /p4mm	106	<i>I</i>			<i>a</i> _{squ} = 3.7 (100)	6.2	1.28	4.8
A10*/4	10* ^j	4	G -8	Col _{squ} /p4mm	94	<i>I</i>			<i>a</i> _{squ} = 3.9 (25)	6.8		5.3
A16/3	16	3	Cr 47	ChL _{hex}	127	<i>I</i>			<i>a</i> = 4.7, <i>c</i> = 4.6 (80)	88.0	1.57	56
A16/4	16	4	Cr 38	ChL _{hex}	122	<i>I</i>			<i>a</i> = 5.0, <i>c</i> = 4.7 (65)	101.8	1.63	62

^a Enthalpy values are shown in the lower lines in italics; the transition temperatures were determined by DSC (second heating scan, 10 K min⁻¹).

^b Abbreviations: Cr = crystalline phase; G = glassy state of the LC phase; Col_{squ} = square columnar phase, the lattice type is additionally given; Col_{hex} = hexagonal columnar phase; ChL_{hex} = hexagonal channeled layer phase; I = isotropic liquid. ^c *a*, *c*, = lattice parameters; *d* = layer spacing. ^d *V*_{cell} = volume of a unit cell (for the columnar phases, a stratum height of *h* = 0.45 nm was assumed).²⁴ ^e *V*_{mol} = molecular volume calculated using the crystal volume increments reported by Immirzi.²⁵ ^f *n*_{cell} = number of molecules per unit cell, calculated as *n*_{cell} = *V*_{cell}/*V*_{mol}; *n*_{cy} = average number of molecules arranged in a stratum around each polar column (only given for the p4gm phases, where four columns are organized in a unit cell, for the p4mm phases; this value corresponds to *n*_{cell}). ^g Two coexisting mesophases, *a*_{squ1} refers to the p4gm phase, *a*_{squ2} refers to the p4mm phase. ^h Structure of this compound is slightly different from the general formula as there is a direct coupling of the CONH group to the aromatic core. ⁱ Values for the ChL_{hex} phase. ^j Racemic 3,7-dimethyloxy chains.

All compounds show enantiotropic (thermodynamically stable) liquid crystalline phases over a broad temperature range. Some compounds do not crystallize even after prolonged storage (> 1 year) and form glassy LC materials at reduced temperature. The mesophase stability and the mesophase types are strongly dependent upon the size of the polar lateral chain and the length of the terminal alkyl chains.

2.1. Effect of the Size of the Lateral Polar Group. Figure 2 shows the dependence of the properties of compounds **A10/n**, having two terminal decyloxy chains, on the length of the oligo(oxyethylene) chain connecting the 1-acylamino-1-deoxy-D-sorbitol unit to the rigid terphenyl core. With increasing length of this chain, the transition temperatures decrease, and three different LC phases are observed: SmA, ChL_{hex}, and Col_{squ}/p4mm.

2.1.1. The SmA Layer Structure. Compound **A10/0**,²⁶ in which the carbohydrate unit is directly coupled to the rigid terphenyl core, shows a simple smectic (SmA) phase, as indicated by the typical texture (fanlike texture and optically isotropic homeotropic alignment after shearing can be seen between crossed polarizers) and X-ray diffraction pattern (layer reflection and diffuse scattering in the wide-angle region).²⁶ In this liquid crystalline phase, the molecules are organized in layers, where the terphenyl units are arranged, on average, perpendicular to the layer planes but without in-plane order. These sublayers are separated by layers of alkyl chains. The

(24) The value *h* = 0.45 nm corresponds to the maximum of the wide-angle scattering in the diffraction pattern.

(25) Immirzi, A.; Perini, B. *Acta Crystallogr., Sect. A* **1977**, *33*, 216–218.

(26) Plehnert, R.; Schröter, J. A.; Tschierske C. *J. Mater. Chem.* **1998**, *8*, 2611–2626.

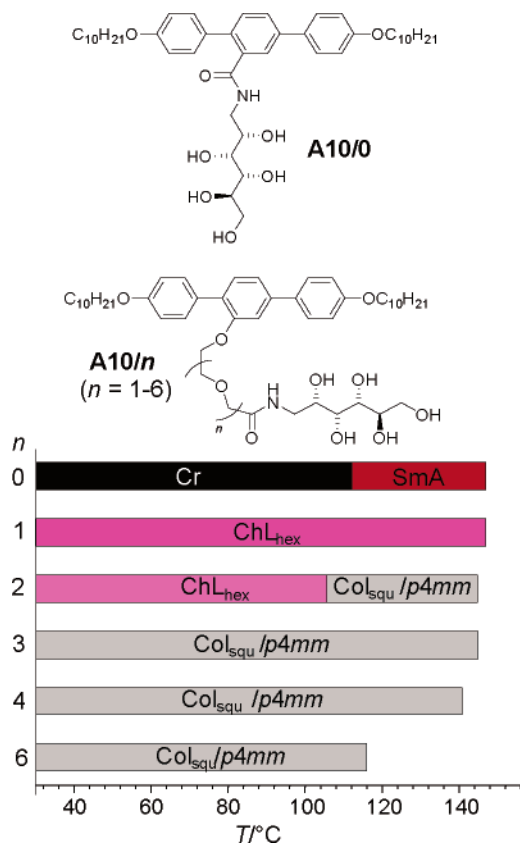


Figure 2. Mesophase types and transition temperatures ($T/^\circ\text{C}$) of compounds **A10/n**, depending on the number of oxyethylene units n . Compound **A10/0**²⁶ is slightly different from the other compounds as the CONH group is directly attached to the aromatic core.

terphenyl layers must also incorporate the lateral carbohydrate units. This is surprising because it can be expected that these bulky groups should strongly disturb such an arrangement. The layer spacing ($d = 3.3$ nm) is significantly smaller than the molecular length. ($L = 4.1$ nm between the ends of the alkyl chains, assuming the most stretched *all-trans* conformation as measured with CPK models, see Figure S2.) This indicates either a high degree of disorder within the layers or a partial intercalation of the alkyl chains. Although it can be expected that the lateral groups, which are normally incompatible with the rigid and lipophilic aromatic cores, would segregate into their own distinct domains, no indication of such domains can be found in the X-ray diffraction pattern. Probably, hydrogen bonding between the polyhydroxy groups and also hydrogen bonding to the π -systems of the aromatic cores and the O atoms of the alkoxy chains have a stabilizing effect upon this layer arrangement, which compensates for the destabilizing steric effects.²⁷

2.1.2. The Hexagonal Channeled Layer Phase. Introduction of the 1,4-dioxapentylene spacer unit between the terphenyl core and the polar group (compound **A10/1**) does not change the isotropization temperature, but it changes the mesophase structure and eliminates the crystalline phase. The mesophase of this compound appears almost completely black between crossed polarizers. Additionally, this mesophase shows a very high viscosity and a viscoelastic response to mechanical stress, indicating a structure with 3D order. In some regions, the texture

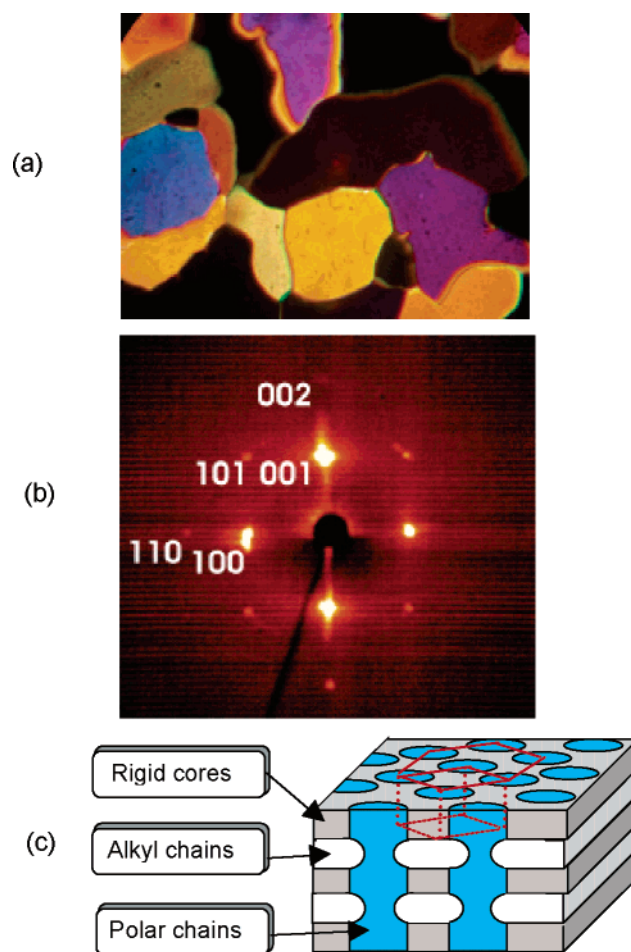


Figure 3. ChL_{hex} phase of **A10/1**: (a) texture of birefringent mosaics as seen between crossed polarizers at 130°C ; (b) X-ray diffraction pattern of an aligned sample of this mesophase at 100°C ; (c) model of the molecular organization in the ChL_{hex} phase.

is characterized by strongly birefringent mosaics (see Figure 3a). All of these observations indicate an optically uniaxial mesophase with a 3D-lattice. The X-ray diffraction pattern of compound **A10/1** shows only diffuse wide-angle scattering, which indicates that this is a liquid crystalline phase. In the small-angle region (see diffraction pattern of an aligned sample in Figure 3b), the positions of the Bragg reflections (001, 100, 101, 110, and 002) indicate a 3D hexagonal lattice ($P6/mmm$) with parameters $a = 4.0$ nm and $c = 3.76$ nm. All of these optical, rheological, and crystallographic data are in line with a hexagonal channeled layer phase (ChL_{hex}). This mesophase was recently investigated in detail, and the structure (Figure 3c) was confirmed by electron density calculations using high-resolution scattering data.¹² Accordingly, this mesophase consists of alternating layers of aromatic units and aliphatic chains, penetrated at right angles by columns with undulating profiles containing the polar lateral groups (Figure 3c). The columns are arranged on a 2D hexagonal lattice. Thus, the structure consists of layers perforated by an array of polar channels. The proposed structure is in complete agreement with the molecular dimensions, as for example the length of an extended molecule of **10/1** ($L = 4.1$ nm) fits very well with the parameter $c = 3.76$ nm.²⁸ The likely reason for the appearance of this unusual

(27) Hildebrandt, F.; Schröter, J. A.; Tschierske, C.; Festag, R.; Kleppinger, R.; Wendorff, J. H. *Angew. Chem., Int. Ed. Engl.* **1995**, *34*, 1631–1633.

(28) This small negative deviation ($d = 0.92L$) is typical for LC phases with a layer structure and is due to conformational disorder of the alkyl chains.

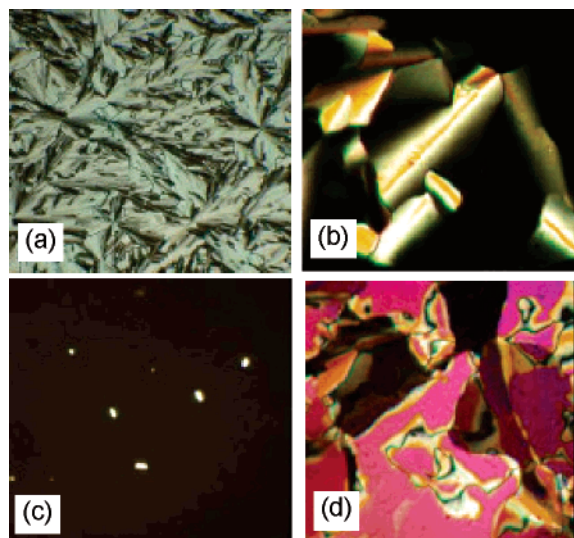


Figure 4. Representative textures of compound **A10/2** as seen between crossed polarizers: (a) $\text{Col}_{\text{sq}}/p4mm$ phase at 142 °C (homogeneous alignment); (b) $\text{Col}_{\text{sq}}/p4mm$ phase at 142 °C (predominately homeotropic alignment); (c) optically isotropic texture of the homeotropically aligned ChL_{hex} phase as obtained by cooling the homogeneously aligned $\text{Col}_{\text{sq}}/p4mm$ phase to 53 °C (same region as a); (d) birefringent texture of the ChL_{hex} phase as obtained by cooling the homeotropically aligned $\text{Col}_{\text{sq}}/p4mm$ phase to 53 °C (same region as b).

mesophase is the enlargement of the incompatible polar lateral group brought about by the introduction of the spacer between the terphenyl core and the carbohydrate unit. This leads to segregation of the lateral groups from the aromatic cores and enables fusion of the polar domains from adjacent layers into infinite polar columns.

2.1.3. The $\text{Col}_{\text{sq}}/p4mm$ Square Cylinder Phase. The mesophase of compounds **A10/3**–**A10/6** and the high-temperature phase of compound **A10/2** show spherulitic textures or filament textures with optically isotropic regions, as shown in Figure 4a,b. This mesophase exhibits a much lower viscosity than the ChL_{hex} phase. All these observations indicate a fluid and optically uniaxial columnar phase. The X-ray diffraction pattern of the aligned mesophase of compound **A10/4** is shown in Figure 5a. In the wide-angle region, a diffuse outer scattering indicates the liquid crystal nature of the phase. In the small-angle region, the sharp reflections (10, 11, and 01) can be indexed on the basis of a $\text{Col}_{\text{sq}}/p4mm$ lattice with the lattice parameter $a_{\text{sq}} = 4.0$ nm.

This diffraction pattern can be explained by the model shown in Figure 5b. Accordingly, the aromatic cores form cylinder shells with a square-shaped cross section enclosing columns containing the segregated lateral polar groups. The nonpolar alkyl chains form columns located at the corners of the squares, running along the edges of the cylinders. These alkyl columns interconnect the cylinder walls.²⁹ The reconstructed electron density map of the $\text{Col}_{\text{sq}}/p4mm$ phase of compound **A10/4** (Figure 5c)¹⁵ confirms this model. It clearly shows the square arrangement of the alkyl columns (low electron density, red regions) and the polar columns (high electron density, blue

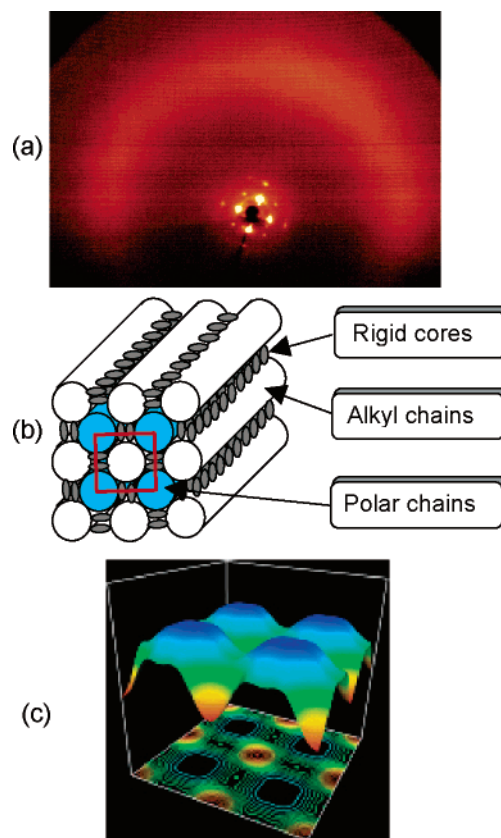


Figure 5. $\text{Col}_{\text{sq}}/p4mm$ phase of compound **A10/4**: (a) X-ray diffraction pattern at 137 °C; (b) model of the $\text{Col}_{\text{sq}}/p4mm$ phase; (c) electron density map of the $\text{Col}_{\text{sq}}/p4mm$ phase¹⁵ (combined surface and contour plot); the blue regions are the high electron density domains (polar columns), and the red regions are the low electron density areas (alkyl chains).

regions). The lattice parameter a_{sq} increases from 3.7 nm for **A10/2** to 4.2 nm for **A10/6**, which indicates that the columns expand to a certain degree and that this expansion is limited by the length of the molecule in the most stretched conformation ($L = 4.1$ nm).

For compound **A10/2**, which has a relatively short lateral chain, a second mesophase has been observed below the $\text{Col}_{\text{sq}}/p4mm$ phase. The typical spherulitic texture of the $\text{Col}_{\text{sq}}/p4mm$ phase (see Figure 4a) breaks up upon cooling at 115 °C, and the whole sample becomes optically isotropic at 102 °C (Figure 4c).³⁰ Under other experimental conditions, the $\text{Col}_{\text{sq}}/p4mm$ phase can be grown with predominately homeotropic alignment (columns predominately perpendicular to the glass surface), characterized by large optically isotropic domains and birefringent filaments (see Figure 4b). If this sample is cooled in the same temperature range between 115 °C and 102 °C, a birefringent mosaic texture develops; i.e., most of the optically isotropic areas become birefringent (Figure 4d). The textural features of this low-temperature phase are very similar to those of the ChL_{hex} phase of compound **A10/1**. In addition, the viscosity of the low-temperature phase is significantly higher than in the Col_{sq} phase. All of these observations suggest that the low-temperature phase should represent a ChL_{hex} phase. (For X-ray data, see Table S1 in the Supporting Information.)³¹

(29) The mesophases reported herein represent ordered *fluids*, which means that there is no long-range order in atomic or molecular positions. Hence, there are no well-defined crystal-like structures, as might be suggested by the schematic models shown. Instead, there are distinct regions with enhanced concentration of aromatic cores, polar groups, and aliphatic chains. Due to this disorder, only diffuse scattering can be found in the wide-angle region of the diffraction pattern.

(30) The transition takes place between 102 °C and 115 °C on heating and cooling, with the DSC peak maximum at $T = 107$ °C; the broadness of the transition might be due to the fact that a 3D ordered mesophase is involved in the transition and that a complete reorganization of the molecules takes place.

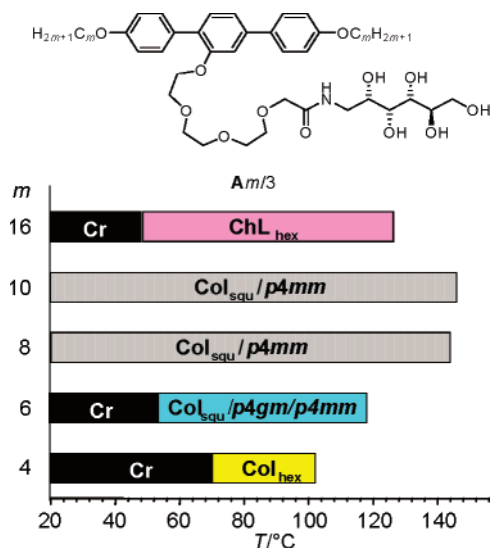


Figure 6. Mesophase types and transition temperatures ($T/^\circ\text{C}$) of compounds $\mathbf{A}m/3$ as a function of the length m of terminal alkyl chains (for $\mathbf{A}6/3$ the $p4gm$ and the $p4mm$ phase coexist over the whole temperature range as indicated by X-ray scattering (see Table S1 of the Supporting Information)).

Hence, as shown in Figure 2, elongation of the polar lateral chain leads to a transition from simple layers via hexagonal channelled layers to a square cylinder structure.

2.2. Influence of the Length of the Terminal Alkyl Chains.

Figure 6 graphically summarizes the dependence of the phase transitions on the length of the terminal alkyl chains for the homologous series of compounds $\mathbf{A}m/3$, which have the polar group connected by a tris(oxyethylene) spacer unit to the p -terphenyl core. As the terminal alkyl chains are reduced from hexadecyl ($\mathbf{A}16/3$) to decyl ($\mathbf{A}10/3$), the mesophase types change from ChL_{hex} to $\text{Col}_{\text{squ}}/p4mm$. Compound $\mathbf{A}6/3$ has two coexisting mesophases, the $\text{Col}_{\text{squ}}/p4mm$ ($a_{\text{squ}} = 3.6$ nm) and another square columnar phase with a $p4gm$ lattice and a much larger lattice parameter ($a_{\text{squ}} = 7.9$ nm). Compound $\mathbf{A}4/3$, with the shortest alkyl chains, forms a hexagonal columnar phase. Hence, with decreasing alkyl chain length, the sequence $\text{ChL}_{\text{hex}} - \text{Col}_{\text{squ}}/p4mm - \text{Col}_{\text{squ}}/p4gm - \text{Col}_{\text{hex}}$ is observed.

A similar sequence of phases was observed for the series of compounds $\mathbf{A}m/4$, having a longer tetra(oxyethylene) spacer unit (see Figure 7). Due to the larger size of the lateral group in compounds $\mathbf{A}m/4$, the lattice parameters are slightly enlarged, and the phase types are shifted to compounds with longer alkyl chain length. For example, compound $\mathbf{A}6/4$ has a uniform $\text{Col}_{\text{squ}}/p4gm$ phase ($a_{\text{squ}} = 8.0$ nm) and a Col_{hex} phase at higher temperature. In addition, compound $\mathbf{A}4/4$ shows a reversible inversion of the birefringence within the temperature range of the Col_{hex} phase at 91°C , which is not found for the related compound $\mathbf{A}4/3$.

2.2.1. The $\text{Col}_{\text{squ}}/p4gm$ Pentagonal Cylinder Phase. The X-ray diffraction pattern of the square columnar phase of compound $\mathbf{A}6/4$ (see Figure 8a) is clearly distinct from those of the $\text{Col}_{\text{squ}}/p4mm$ phases. There are numerous small-angle reflections, which can be indexed to a square lattice of the plane group $p4gm$. The calculated lattice parameter is $a_{\text{squ}} = 8.0$ nm

(31) In addition, these changes in texture indicate that the direction of the polar columns with respect to the surfaces changes at the phase transition $\text{Col}_{\text{squ}}/p4gm$ to ChL_{hex} , either from parallel to perpendicular (Figure 5 a to c) or from perpendicular to parallel (Figure 5 b to d).

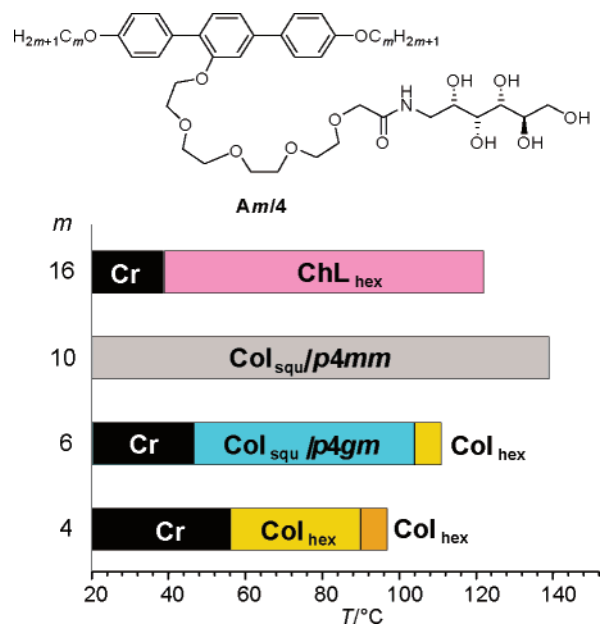


Figure 7. Mesophase types and transition temperatures ($T/^\circ\text{C}$) of compounds $\mathbf{A}m/4$ as a function of the length of terminal alkyl chains. The Col_{hex} phases have either negative (bright yellow) or positive (dark yellow) birefringence; in compound $\mathbf{A}4/4$, a change of the sign of birefringence is seen within the temperature range of the Col_{hex} phase.

($T = 98^\circ\text{C}$); this value is about twice as large as that observed for the $\text{Col}_{\text{squ}}/p4mm$ phases (see Table 1). This parameter is also more than twice as large as the molecular length ($L = 3.1$ nm), and this excludes a simple square cylinder structure. About 25 to 26 molecules are arranged in a unit cell with a height of 0.45 nm.²⁴ This $\text{Col}_{\text{squ}}/p4gm$ phase is also made up of cylinders, but in this case with a pentagonal cross-sectional shape. The polar lateral chains fill the interior of these cylinders, and the columns of the alkyl chains interconnect the cylinder walls. These pentagonal cylinders can only organize in a regular and periodic way if they form cylinder pairs (indicated by dotted green lines in Figure 8b). These pairs have symmetry higher than that of the individual pentagonal cylinder and adopt a 90° turn herringbone-like packing, leading to the $p4gm$ -lattice.

The proposed pentagonal cylinder structure of the $\text{Col}_{\text{squ}}/p4gm$ phase was confirmed by electron density calculations based on high-resolution powder X-ray diffraction pattern (synchrotron X-ray source). In the electron density map (see Figure 8c), the high electron density regions (polar chains, shown in blue and purple) form pentagons that are separated by squares and triangles of low electron density (yellow to red color), containing the alkyl chains.¹³ The network of terphenyl cores can be regarded as a pentagonal net interconnected by threefold and fourfold nodes (columns of alkyl chains). The interior of the cylinder frame is filled by the polar columns.²⁹

2.2.2. Hexagonal Columnar Phases: Columns In An Ordered Continuum. Extending the polar chain (see Table 1, compounds $\mathbf{A}6/n$), raising the temperature (compounds $\mathbf{A}4/2$, $\mathbf{A}6/4$, and $\mathbf{A}6/5$), or reducing the alkyl chain length in both $\mathbf{A}m/3$ and $\mathbf{A}m/4$ series leads to a transition from square to hexagonal columnar phases. The change in birefringence pattern at the $\text{Col}_{\text{squ}}/p4gm$ to Col_{hex} phase transition of compound $\mathbf{A}6/4$ is shown in Figure 9a. The texture itself does not change, but the phase transition can be detected by a slight decrease in

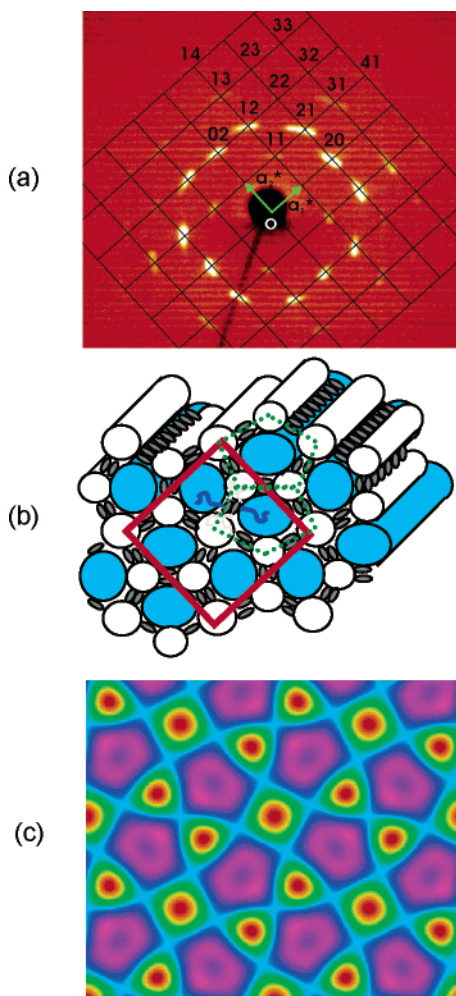


Figure 8. $\text{Col}_{\text{sq}}/p4gm$ phase of compound A6/4: (a) X-ray diffraction pattern of an aligned sample of the $\text{Col}_{\text{sq}}/p4gm$ phase¹³ at 98 °C; (b) model of the $\text{Col}_{\text{sq}}/p4gm$ phase: blue columns incorporate the polar lateral groups, white columns incorporate the alkyl chains interconnecting the terphenyl units at the nodes; (c) electron density map of the $\text{Col}_{\text{sq}}/p4gm$ phase; the high electron density regions (polar chains) are shown in blue and purple and low electron density regions (alkyl chains) in yellow to red.¹³

birefringence. X-ray diffraction confirms a 2D hexagonal lattice (see Figure 9b), but the lattice parameter ($a_{\text{hex}} = 4.3$ nm) is significantly smaller than expected for the hexagonal cylinder structure shown in Figure 10a. The expected value of the lattice parameter for this structure should correspond to the diameter of the cylinder inscribed in the hexagonal frame and can be calculated according to $2r_{\text{hexagon}} = a_{\text{hex,calc}} = 3^{1/2}L = 5.36$ nm, using the molecular length $L = 3.1$ nm (most stretched conformation). Furthermore, it is remarkable that the phase transition enthalpy of the transition $\text{Col}_{\text{sq}}/p4gm$ to Col_{hex} ($\Delta H = 1.6$ kJ mol⁻¹) is higher than that of the Col_{hex} to isotropic transition ($\Delta H = 0.7$ kJ mol⁻¹, see Table 1). This indicates that a significant change takes place at the $\text{Col}_{\text{sq}}/p4gm$ to Col_{hex} transition. Because this transition is induced either by raising the temperature or by reducing the alkyl chain length, it is reasonable to assume that the segregation of the aromatic cores from the alkyl chains is lost or strongly reduced at the transition into this Col_{hex} phase. Indeed, in the electron density map shown in Figure 9c, a nearly constant electron density within the low electron density region (yellow to red) around the high electron density columns (blue to pink, polar groups) can be seen, which confirms the above assumption. Another notable observation

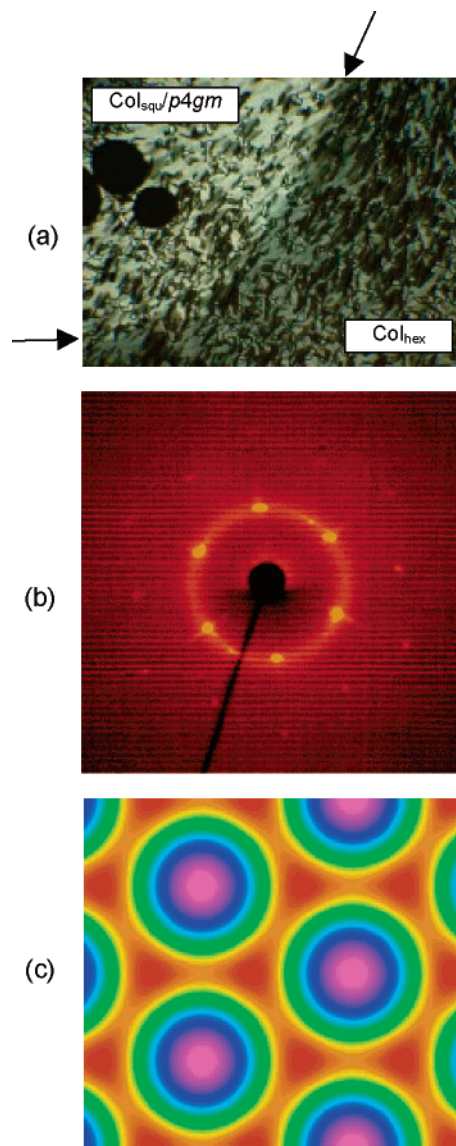


Figure 9. Hexagonal columnar phase of compound A6/4: (a) transition from the $\text{Col}_{\text{sq}}/p4gm$ phase (upper left) to the Col_{hex} phase (lower right) observed at 104 °C (the black regions are air bubbles; arrows indicate the borderline between the two phases); (b) small-angle range of the X-ray diffraction pattern of an aligned sample at 106 °C; (c) electron density map calculated from synchrotron X-ray data at $T = 108$ °C; high electron density regions (polar chains) are shown in blue and purple, and low electron density regions (alkyl chains plus aromatic cores) are shown in yellow to red.

is that, at the $\text{Col}_{\text{sq}}/p4gm$ to Col_{hex} phase transition, the defect structure (i.e., the optical textures) remains unchanged. This indicates that during this phase transition, the polar columns retain their orientation. Furthermore, there is only a slight decrease in birefringence, indicating that the orientation of the terphenyl units does not change fundamentally (see Figure 9a). Hence, in the Col_{hex} phase, the terphenyl units should, on average, align nearly perpendicular to the column axis, as in the $\text{Col}_{\text{sq}}/p4gm$ phase. Had the orientation of the terphenyl units changed completely with respect to the column axis, aligning parallel to it, the sign of the birefringence would have changed at the phase transition, and consequently, the birefringence would have passed through zero. Evidently, this was not the case. Nevertheless, the reduction in birefringence at the $\text{Col}_{\text{sq}}/p4gm$ to Col_{hex} phase transition indicates a reduction in orientational order of the terphenyl units or an increasing tilt

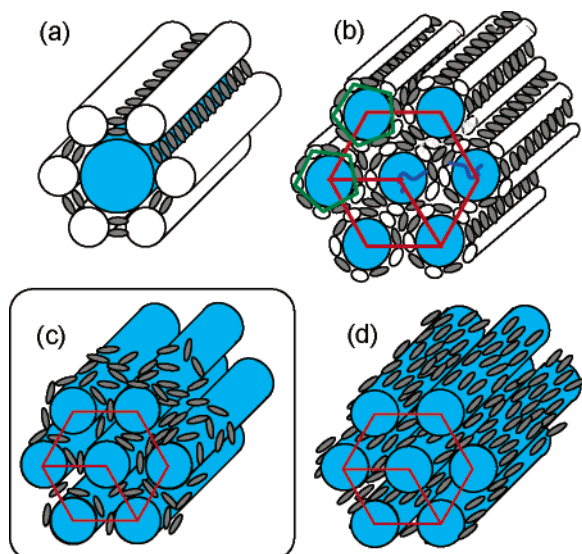


Figure 10. Possible models of molecular organization in the Col_{hex} phases of compounds Am/n arranged from (a) to (d) in the order of decreasing segregation between aromatic cores and aliphatic chains; white columns contain alkyl chains, blue columns, the polar lateral groups, and the rigid cores are shown in gray. (a) Hexagonal honeycomb cylinder net (only one cylinder is shown, aliphatic chains and aromatic cores are segregated); (b) rotationally disordered pentagonal cylinders (each polar cylinder is framed by five aromatic blocks in a stratum—within the cylinder shells, the aromatic and aliphatic moieties are segregated, but there is no interconnection of the aliphatic columns belonging to adjacent cylinders; a related structure is also possible with hexagonal cylinders); (c) hexagonal organization of columns in a continuum of terphenyl and alkyl chains, where the terphenyls are arranged tangentially around the columns with the long axis perpendicular to the columns; this arrangement requires the presence of some residual segregation in the form of cybotactic clusters of cylinder shells as shown in (b); (d) hexagonal organization of columns in a nematic continuum of terphenyl and alkyl chains, where the terphenyls are arranged parallel to the columns; this organization is favored by the minimization of the excluded volume.

toward the column axis. Further information concerning the phase structure was obtained from the investigation of the Col_{hex} phase in compound **A4/4**.

Compound **A4/4** (see Figure 7) shows an inversion of birefringence within the temperature range of the Col_{hex} phase. Upon heating, at 91 °C, the birefringent texture (Figure 11d) becomes completely dark between crossed polarizers (Figure 11b). In a thick sample, distinct domains with blue and red interference color can be distinguished (see Figure 11c), which result from the wavelength dependence of the refractive indices, a very typical feature of birefringence inversion.³² Upon further heating, the birefringence increases again until the clearing temperature is reached (Figure 11a). The sign of the birefringence of the Col_{hex} phase was experimentally determined by examining the texture between crossed polarizers. At first, monodomains of the sample were oriented with the columnar axis at 45° to the crossed polarizers. A first-order λ -plate was placed with the direction of n_{α} (smaller refractive index) parallel to the columnar axis. In the optically isotropic state at 91 °C, the sample adopts the red interference color of the λ -plate. Below 91 °C, the domain becomes blue. This indicates that in the low-

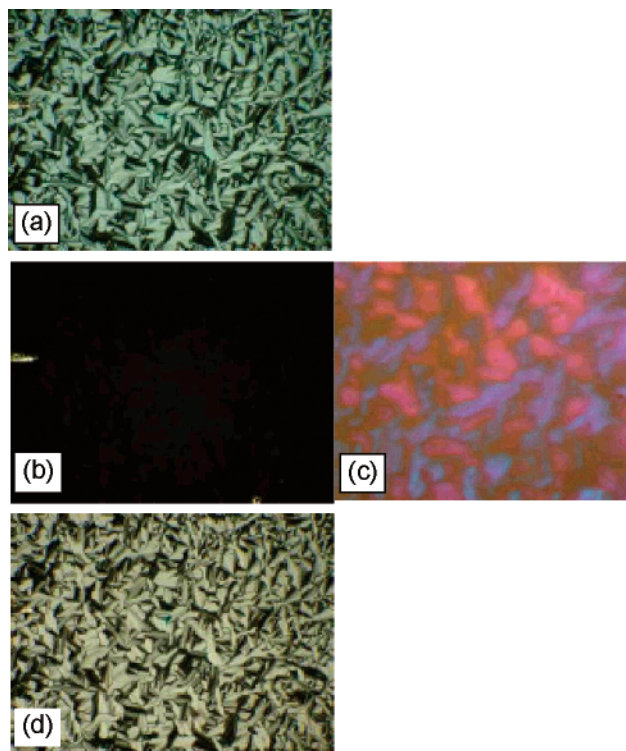


Figure 11. Textures of the Col_{hex} phase of compound **A4/4** at different temperatures: (a) birefringent texture at 95 °C; (b) optically isotropic state at 91 °C; (c) thick sample as observed at 91 °C with polychromatic light between crossed polarizers and with prolonged exposure time (ca. fivefold magnification with respect to a, b, and d); (d) birefringent texture at 87 °C.

temperature columnar phase n_{\parallel} is smaller than n_{\perp} ($n_{\parallel} < n_{\perp}$, where n_{\parallel} and n_{\perp} are the refractive indices parallel and perpendicular to the polar columns, respectively). In other words, below 91 °C, the birefringence of the Col_{hex} phase is negative. Above 91 °C, the domain becomes yellow, indicating that the birefringence is positive. The birefringence inversion is completely reversible, but no transition enthalpy is found at 91 °C, and also, no significant change can be detected in the X-ray diffraction pattern. The observed inversion in birefringence can be explained in the following way: In the continuum between the polar cylinders, there is preferred parallel (“nematic-like”) alignment of the terphenyl cores. On the other hand, at lower temperature, the terphenyl cores are aligned predominately perpendicular to the polar columns, as shown in Figure 10c. Because the birefringence of the phase is determined primarily by the orientation of the terphenyl units with respect to the columns, i.e., the optic axis, this mesophase has negative birefringence.

The vacillating alignment of terphenyl mesogens in the Col_{hex} phase is an indication of the frustration caused by two opposing tendencies: one for the alkyl chains to phase separate in discrete columns (Figure 10b), and the other to forego such separation and maximize the interaction between mesogens by allowing them to form a nematic-like continuum (Figure 10d). The latter tendency prevails; i.e., microphase separation is abandoned and nematic-like alignment achieved in **A4/4**, the compound with the shortest alkyl chains, as would be expected. The “transition” between mesogen alignments perpendicular and parallel to the polar columns suggests an analogy with the upper critical dissolution point in macroscopically immiscible liquids. It thus seems that segregation of aromatic and aliphatic parts may not

(32) There are only a few examples of inversion of birefringence in LC systems: (a) Pelzl, G.; Sackmann, H. *Mol. Cryst. Liq. Cryst.* **1971**, *15*, 75–87. (b) Zimmermann, H.; Poupko, R.; Luz, Z.; Billard, J. *Z. Naturforsch.* **1986**, *41a*, 1137–1140. (c) Ungar, G.; Abramic, D.; Percec, V.; Heck, J. *Liq. Cryst.* **1996**, *21*, 73–86. (d) Reiffenrath, V.; Bremer, M. *Abstr. Pap. Am. Chem. Soc.* **1999**, *218*, 70-ORGN. (e) Olssen, N.; Dahl, I.; Helgee, B.; Komitov, L. *Liq. Cryst.* **2004**, 1555–1568.

be completely lost at the Col_{sq} to Col_{hex} transition, and locally, residues of the cylinder shells remain. If present, such residual pentagonal or hexagonal clusters³³ would be rotationally disordered around the polar columns. (Hence, the real structure is probably somewhere between the models b and c shown in Figure 10.) Upon heating, these clusters decrease in size, and the excluded volume effect becomes more dominating, giving rise to an average alignment of the terphenyls closer to parallel to the column axis, leading to positive birefringence. Because the inversion of birefringence is not associated with a distinct first-order phase transition, it seems that the reorganization of the terphenyl units is a phenomenon similar to the formation of cybotactic clusters found in some nematic phases close to the Sm-to-N transition.³⁴ In contrast to most cybotactic N phases, which exist only over short temperature ranges, in the Col_{hex} phases reported herein, the cybotactic behavior is predominant; i.e., no real parallel organization of terphenyls and polar columns (as shown in Figure 10d) is reached before the transition to the isotropic state.

The hexagonal columnar phases of compounds **A4/2**, **A4/3**, **A6/4**, **A6/5**, and **A6/6** should all have the same structure with a perpendicular organization of columns and terphenyls, as additionally proven for that of compound **A6/6** by X-ray experiments with aligned samples. (The maxima of the diffuse wide-angle scatterings are located on the equator; see Figure S1 in the Supporting Information.) However, a change in the sign of birefringence, as found for **A4/4**, was not observed for any of these Col_{hex} phases. Only for compound **A4/3**, which has one oxyethylene unit less than **A4/4**, is a continuous decrease in birefringence with increasing temperature observed, but apparently in this case no reversal in birefringence occurs before isotropization.

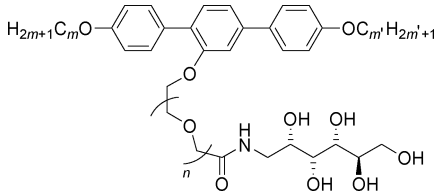
2.3. Other Variations of the Molecular Structure.

2.3.1. Branched Alkyl Chains. Compounds **A10*/3** and **A10*/4** (see Table 1) with branched decyl chains (3,7-dimethyloctyloxy chains) show $Col_{sq}/p4mm$ phases the same as those of the corresponding linear derivatives **A10/3** and **A10/4** with the same number of C-atoms. It seems that this structural variation slightly reduces the clearing temperatures, whereas the mesophase type is not changed.

2.3.2. Nonequal Terminal Chains. Compounds **A6.16/n** and **A16.6/n** comprise two different terminal alkyl chains at the ends of the *p*-terphenyl units, see Table 2. For all six compounds, only the $Col_{sq}/p4mm$ phase was observed, irrespective of the position of the longer chain relative to the lateral group. Also, the mesophase stability of the two sets of isomeric compounds **A6.16/n** and **A16.6/n** is nearly the same as that of similar compounds with identical end chains of comparable total length (e.g., compounds **A10/n**).

2.3.3. Position of the Lateral Chain (Y-Shaped Amphiphiles). The two compounds **B10/n** with a polar chain at the peripheral 3-position show only the $Col_{sq}/p4mm$ phase, see Table 3. Comparison with the corresponding centrally substi-

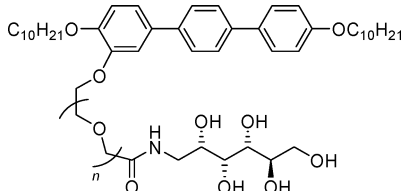
Table 2. Mesophases, Phase Transition Temperatures, Phase Transition Enthalpies, and Lattice Parameters of the Facial Amphiphiles **A6.16/n** and **A16.6/n**^a



compd	<i>m</i>	<i>m'</i>	<i>n</i>	<i>T</i> ^o C		<i>a</i> _{sq} /nm (<i>T</i> ^o C)
				<i>ΔH</i> /kJ·mol ⁻¹		
A6.16/3	6	16	3	Cr 51	<i>Col_{sq}/p4mm</i>	137 I
				49.6	2.3	4.2 (90)
A6.16/4	6	16	4	Cr 52	<i>Col_{sq}/p4mm</i>	135 I
				42.3	2.5	4.4 (90)
A6.16/6	6	16	6	Cr 56	<i>Col_{sq}/p4mm</i>	120 I
				50.3	2.4	4.5 (80)
A16.6/3	16	6	3	Cr 49	<i>Col_{sq}/p4mm</i>	138 I
				50.3	2.6	4.2 (80)
A16.6/4	16	6	4	Cr 43	<i>Col_{sq}/p4mm</i>	134 I
				38.7	2.9	4.2 (95)
A16.6/6	16	6	6	Cr 32	<i>Col_{sq}/p4mm</i>	119 I
				51.3	3.0	4.4 (95)

^a Enthalpy values are given in the lower lines in italics.

Table 3. Mesophases, Phase Transition Temperatures, Phase Transition Enthalpy Values, and Lattice Parameters of the Facial Amphiphiles **B10/n**^a



compd	<i>n</i>	<i>T</i> ^o C		<i>a</i> _{sq} /nm (<i>T</i> ^o C)
		<i>ΔH</i> /kJ·mol ⁻¹		
B10/3	3	Cr 117	<i>Col_{sq}/p4mm</i>	155 I
		48.9	4.1	4.1 (90)
B10/4	4	Cr 114	<i>Col_{sq}/p4mm</i>	154 I
		66.9	5.6	4.2 (100)

^a Enthalpy values are given in the lower lines in italics.

tuted (2'-substituted) compounds **A10/3** and **A10/4** shows that changing the position of the lateral chain does not change the mesophase type. The $Col_{sq}/p4mm$ phase is slightly more stable in the former compounds; their isotropization temperatures are 10 °C higher, but because the melting points are also increased, the overall mesophase range is actually reduced. This slight increase in clearing temperature might be due to a less serious steric destabilizing effect of the peripheral substituent in compounds **B10/n** or to a change in conformation of the *p*-terphenyl unit (reduction of the twist of the terphenyl core).³⁵

2.4. Solvent-Induced Mesophases: New Types of Laminated Mesophases. Actually, all the compounds discussed above are amphotropic liquid crystals¹⁷ because their mesomorphic properties can be influenced by specific interaction of appropriate solvents with one of the incompatible units: lipo-

(33) The measured parameter $a_{hex} = 4.3$ nm (compound **A6/4**) is only slightly larger than the calculated diameter of a cylinder inscribed in a regular pentagon formed by these molecules ($2r_{pentagon} = 4.2$ nm). Also the number of molecules arranged around the columns n_{cyl} (see Table 1) does not change at the phase transition, assuming an unchanged 0.45-nm stratum thickness of the column; moreover, n_{cyl} becomes even slightly smaller in some cases (compound **A4/2**). This suggests that the pentagonal shape remains, but the pentagonal cylinders become rotationally disordered.

(34) De Vries, A. *Mol. Cryst. Liq. Cryst.* **1970**, *10*, 219–236.

(35) (a) Gray, G. W.; Hird, M.; Toyne, K. J. *Mol. Cryst. Liq. Cryst.* **1991**, *195*, 221–237. (b) Hird, M.; Toyne, K. J.; Hindmarsh, P.; Jones, J. C.; Minter, V. *Mol. Cryst. Liq. Cryst.* **1995**, *260*, 227–240. (c) Andersch, J.; Tschierske, C.; Diele, S.; Lose, D. *J. Mater. Chem.* **1996**, *6*, 1297–1307. (d) Kölbl, M.; Beyersdorff, T.; Tschierske, C.; Diele, S.; Kain, J. *Chem.-Eur. J.* **2000**, *6*, 3821–3837.

philic solvents can swell the nonpolar regions, and polar solvents can swell the polar regions.

Formamide can form hydrogen bonds with the poly(oxyethylene) chains as well as with the OH groups and the amide group of the lateral chain; i.e., it interacts specifically with the polar lateral chains. The influence of formamide upon the Col_{hex} mesophases of compound **A4/4** was investigated by means of the solvent-penetration technique. The mesophases developing in the contact region between the amphiphile and the solvent were recorded qualitatively by polarizing microscopy. Panels a and b of Figure 12 display the contact region of **A4/4** with formamide at different temperatures and panel e is a sketch of the binary phase diagram, as recorded on cooling. With an increasing concentration of formamide, the original Col_{hex} phase of pure **A4/4** was destabilized, and new types of mesophases were made to appear. In the contact region, on cooling from the isotropic state, a texture with homeotropic alignment and some defects (small crosses and oily streaks) is formed, which is typical of SmA phases (Figure 12a). This solvent-induced SmA phase is separated from the Col_{hex} phase of the pure compound **A4/4** by an isotropic liquid ribbon. By further cooling, a schlieren texture with strong birefringence grows in the center of the homeotropic SmA domain (Figure 12b). This indicates the formation of an optically biaxial mesophase. Crystallization occurs at 53 °C, and reheating gives a melting point of approximately 77 °C; i.e., the biaxial mesophase is only monotropic, which has inhibited a more detailed investigation. The schlieren texture of this mesophase comprises two brush disclinations, which excludes a synclinic-tilted SmC phase. However, the overall appearance of this mesophase is similar to the textures of the SmA_b phases³⁶ and also to those of the Lam_N phases, which were recently reported for bolaamphiphiles with large lateral semiperfluorinated alkyl chains (see Figure 1).^{10b,c,11} The model proposed for the bolaamphiphiles might also be applicable to the solvent-induced phases of compound **A4/4**. The effect of formamide is to increase the effective size of the polar parts of the molecule by coordinating its molecules to the polar groups. This leads to fusion of the rows of polar columns into infinite layers. In the resulting layer structure, the alkyl chains and the *p*-terphenyl cores are segregated into common layers, whereas the polar parts of the molecules, together with the solvent, form the second set of layers. At high temperature, there is no in-plane order in the apolar layers (Lam_{iso} phase, see Figure 12c) but on cooling, the *p*-terphenyl cores adopt orientational order, which gives rise to the characteristic birefringent schlieren texture. Accordingly, this mesophase can be regarded as a biaxial smectic mesophase (SmA_b -like) or as a laminated nematic phase (Lam_N , see Figure 12d). Although these experiments are only preliminary, they show that it is possible, with these facial amphiphiles, to obtain laminated mesophases similar to those observed for the bolaamphiphiles with lipophilic lateral chains.^{10b,c,11}

Summary and Conclusions

In this investigation, five complex supramolecular LC phases and two solvent-induced LC phases were found for a series of rodlike facial amphiphiles with carbohydrate headgroups. As summarized in Figure 13, a phase sequence $\text{SmA} - \text{ChL}_{\text{hex}} -$

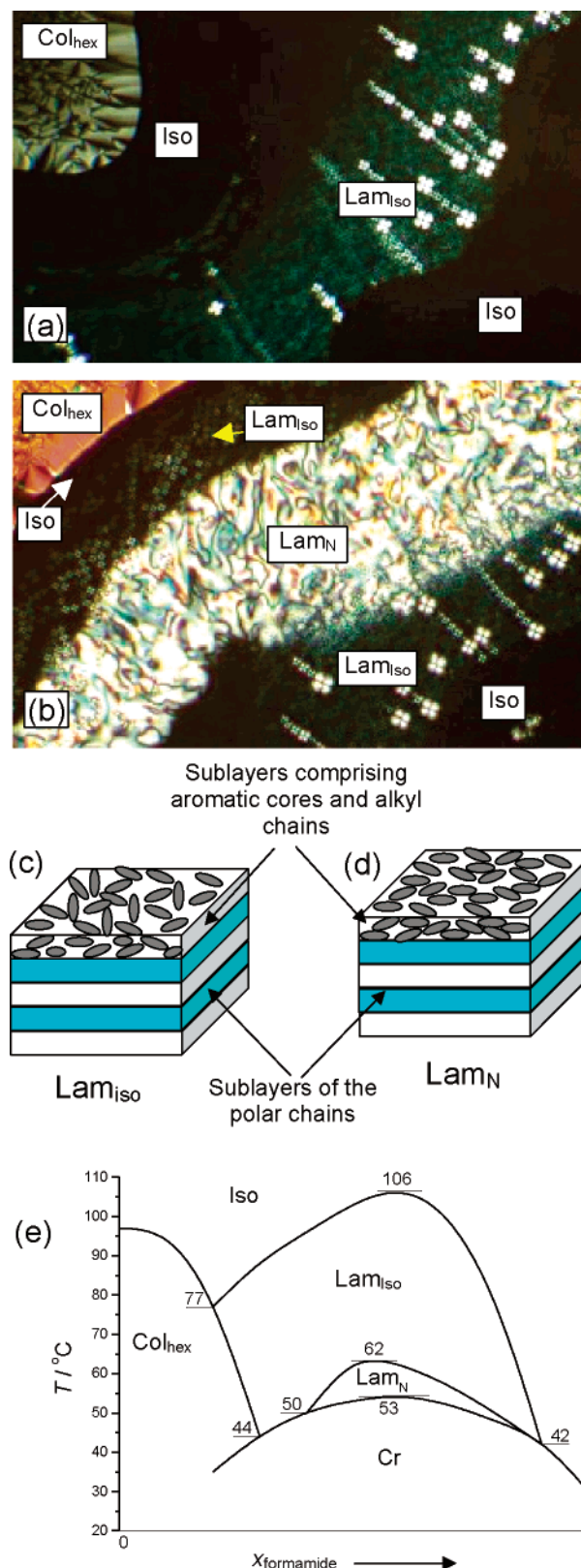


Figure 12. Contact region of **A4/4** (top left) and formamide (bottom right) as observed on cooling between crossed polarizers: (a) at 99 °C; (b) at 61 °C; (c) model of Lam_{iso} phase; (d) model of Lam_N phase; (e) sketch of the nonequilibrium binary phase diagram **A4/4** + formamide as determined by polarizing microscopy of the contact region on cooling (two-phase regions not shown).

$\text{Col}_{\text{sq}}/p4mm - \text{Col}_{\text{sq}}/p4gm - \text{Col}_{\text{hex}} - \text{Lam}_N - \text{Lam}_{\text{iso}}$ has been observed by increasing the volume fraction of the lateral

(36) Hegmann, T.; Kain, J.; Diele, S.; Pelzl, G.; Tschierske, C. *Angew. Chem., Int. Ed.* **2001**, *40*, 887–890.

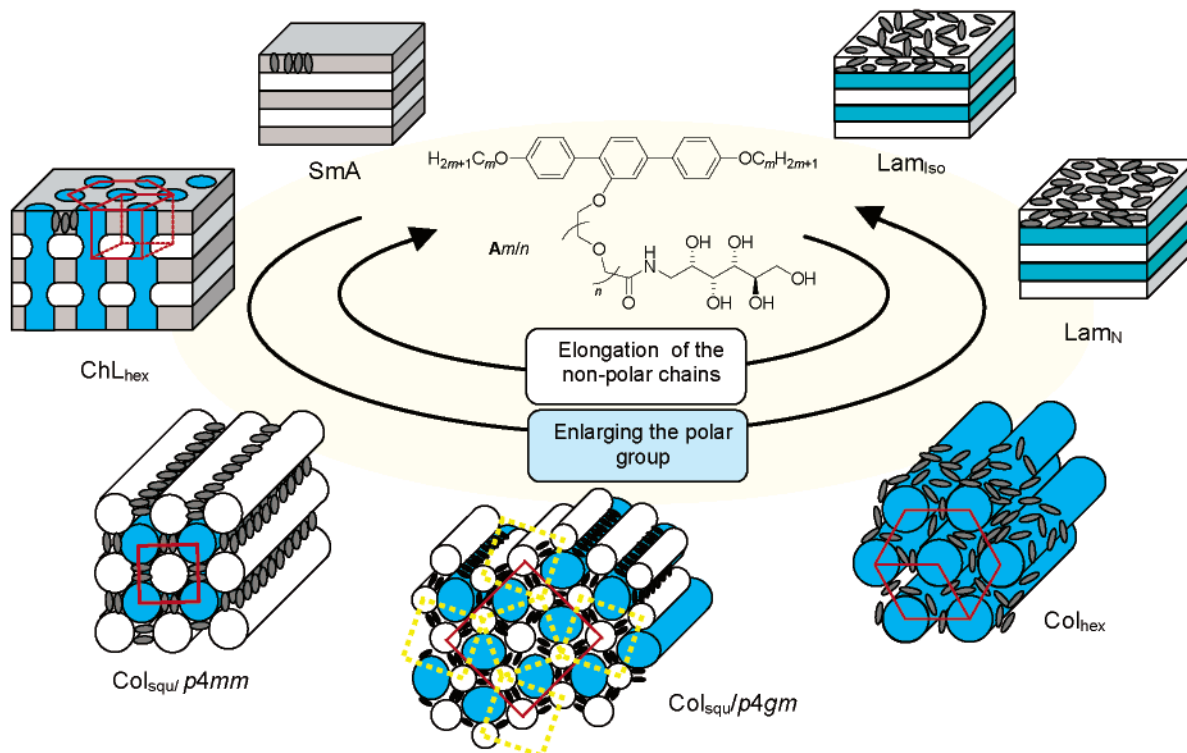


Figure 13. Schematic view of the phase sequence of the facial amphiphiles with lateral polyhydroxy groups as a function of the size of polar lateral and lipophilic terminal groups (Lam_N and Lam_{iso} are proposed for the solvent-induced mesophases).

polar chain or by reducing the volume fraction of the terminal lipophilic chains. Some of the phase transitions are temperature- or solvent-induced.

This sequence of mesophases bears a relation to that found for the bolaamphiphiles $1/n$ with nonpolar lateral chains, shown in Figure 1.¹⁰ Starting with a conventional SmA phase by increasing the volume fraction of the lateral chain at first cylinder structures are formed, which then change into new lamellar phases. This similarity indicates the generality of the self-organization principles involved. Both series of compounds represent ternary amphiphiles with a T-like shape in which a rigid core of defined length is combined with two terminal chains and one lateral chain, incompatible with each other. For the columnar mesophases, the rigid-rod segments tend to restrict the side length of the polygons within relatively narrow limits, giving rise to columns with a well-defined polygonal shape. The lateral chains fill the interior of the polygons; the terminal chains form the corners of these polygons and connect the rigid rods. Thus, the number of sides of the polygons critically depends on the volume of the lateral chain and the length of the molecule. The polygon that provides the exact volume required by the lateral chains is selected. The most remarkable cylinder phase is that built up by pentagonal cylinders ($\text{Col}_{\text{sq}}/p4gm$). It is known that regular pentagons (with identical sides and angles) cannot tile the plane,³⁷ but the LC state, combining order and mobility, enables a slight deviation of the angles and side lengths, which is essential for the formation of the observed honeycomb-like periodic network composed exclusively of pentagonal cylinders.^{38–40}

However, self-assembly of these two classes of compounds also shows major differences, mainly due to the different

positions of the amphiphilic groups. Therefore, the positions of the polar and nonpolar columns in the LC structures are also exchanged, as can be seen, for example, by comparing the $\text{Col}_{\text{sq}}/p4mm$ phase in Figure 1 (bolaamphiphiles) with that shown in Figure 13 (facial amphiphiles). The two $\text{Col}_{\text{sq}}/p4mm$ phases are reversed with respect to the position of the polar columns. The latter serve either as wall-interconnecting columns or as framed columns. Hence, the two $\text{Col}_{\text{sq}}/p4mm$ structures are assigned as color isomers. Because the regions with the strongest cohesive forces (hydrogen bonding) have a different position with respect to the rigid cores, some mesophases are missing in facial amphiphiles, whereas others, not found in bolaamphiphiles $1/n$,¹⁰ emerge (e.g., the ChL_{hex} phase and the noncylinder Col_{hex} phase).

In bolaamphiphiles, the strongest cohesive forces are located at the ends of the molecules, which leads to a dominance of cylinder structures ranging from rhombuses via squares, hexagons, to giant cylinder structures. In the series of facial amphiphiles, these giant cylinder structures are missing. In the case of facial amphiphiles, the phase-separation tendency of the aliphatic groups is relatively weak, and separate aliphatic columns from the aromatic cores only for alkyl length $m \geq 6$. In contrast, in the case of bolaamphiphiles $1/n$, even the relatively short 2,3-dihydroxypropyl units provide sufficient

(38) There is only one report about a pentagonal net in solid crystal structure, but in this case the net deviates from planarity (wavelike deformation) in order to allow for periodic tiling by identical pentagons: Moulton, B.; Lu, J.-J.; Zaworotko, M. J. *J. Am. Chem. Soc.* **2001**, *123*, 9224–9225.

(39) Examples of supramolecular pentagons: (a) Hasenkopf, B.; Lehn, J.-M.; Boumediene, N.; Dupont-Gervais, A.; Dorsselaer, A. V.; Kneisel, B. O.; Baum, G.; Frenske, D. *J. Am. Chem. Soc.* **1997**, *119*, 10956. (b) Campos-Fernandez, C. S.; Clerac, R.; Koomen, J. M.; Russell, D. H.; Dunbar, K. R. *J. Am. Chem. Soc.* **2001**, *123*, 773–776.

(40) Fivefold symmetry in quasi-crystal lattices: Caspar, D. L. D.; Fontano, E. *Proc. Natl. Acad. Sci. U.S.A.* **1996**, *93*, 14271–14278.

(37) Grünbaum, B.; Shephard, G. C. *Tilings and Patterns*; W. H. Freeman: New York, 1987.

tendency for separation to maintain the cylinder structure for a wide variety of different molecules.

In the series of facial amphiphiles reported herein, the $\text{Col}_{\text{sq}}/p4mm$ cylinder phase is the dominant mesophase, found in most compounds. At the same time, in the series of bolaamphiphiles, the $\text{Col}_{\text{hex}}/p6mm$ cylinder phase is dominant, and the $\text{Col}_{\text{sq}}/p4mm$ phase was found for only one compound in a small temperature range.^{10b} This appears to be due to the different length of the rigid cores in the two series of compounds (biphenyl vs terphenyl) and the different size of the end-groups. The size of the lateral polar group of the facial amphiphiles is not sufficient to fill the space inside a hexagon of six terphenyl units. Also, the structure of the pentagonal cylinder phase is slightly different in the two series. In bolaamphiphiles, there is an additional slight deformation of the pentagons (all angles are different), leading to the reduced phase symmetry $\text{Col}_{\text{rec}}/p2gg$ ¹⁰ as compared to that of $\text{Col}_{\text{sq}}/p4gm$ in facial amphiphiles. Possibly, the alkyl and perfluoroalkyl chains,⁴¹ which are more rigid than the oligo(oxyethylene) chains,⁴² might give rise to the additional deformation of the pentagons.

The most striking feature is that the pentagonal cylinder structure is the largest of the stable cylinder structures, and the hexagonal cylinder structure could not be obtained with the compounds investigated herein. The likely reason is that the approach used, which is based on the reduction of the terminal alkyl chain length, also reduces the incompatibility of these chains with the aromatic cores. Therefore, in the hexagonal columnar phases, the terphenyl cores and the alkyl chains are not segregated. However, a parallel organization of the rodlike cores remains, and cybotactic groups (residues of the cylinder structure) keep the terphenyl cores in a predominately perpendicular orientation with respect to the polar columns. This phase has a unique structure, where columns are hexagonally organized in an anisotropic matrix with a local nematic-like order of the terphenyls, and the nematic director changes tangentially around the columns.⁴³ It is a new mesophase, which in some respect can be regarded as complementary to the so-called “tubular–nematic–columnar phase” reported by Saez et al. for laterally appended polyepides.⁴⁴ The latter type of Col_{hex} (and also Col_{rec}) phases is formed by oligomesogens composed of rodlike phenylbenzoate cores with terminal alkyl chains at both ends and lateral alkyl chains that are connected to an oligosiloxane branching point. In the mesophases of these compounds, the oligosiloxane units form columns and the rodlike phenylbenzoate cores with the terminal alkyl chains form a nematic continuum between them. In contrast to the Col_{hex} phases reported here, the nematic director is parallel or only slightly tilted to the columns (similar to Figure 10d).

In addition, there is a much larger variety of different phases in the present facial amphiphiles. For example, as the alkyl length of $m = 16$ is reached, the chains are sufficiently long to

form layers rather than columns, resulting in the ChL_{hex} phase being the “tubular smectic” counterpart of the “tubular nematic” phase.

The columnar cylinder phases ($p4mm$ and $p4gm$), the non-cylinder Col_{hex} phase, and the ChL_{hex} phase reported herein represent new channel structures that might be of practical interest. The polar columns are formed by oligo(oxyethylene) chains that have been widely used as a medium for ion conduction.⁴⁵ In the reported mesophases, the ion conductive channels are one-dimensional and located in a well-structured lipophilic surrounding. These ordered soft-matter systems can easily be organized at interfaces or modulated by electric fields and guest molecules, allowing the preparation of well-defined structures incorporating monodomains of such mesophases. These fluid systems formed in the self-assembly process can then be fixed by cross-linking, polymerization (using slightly modified molecules or additives), or vitrification to obtain stable, functional nanodevices.

In summary, the concept of ternary amphiphilic T-shaped molecules provides a powerful design principle for new and unexpected complex liquid crystalline superstructures. There is an analogy with the approaches used in polymer systems (star-shaped multiblock copolymers^{46,47} and hairy rods^{48,49}) with the difference that the LC structures have lower viscosity, higher perfection, and a smaller (3–30 nm) length scale than those of polymers. Hence, they are much easier to produce in a fast thermodynamically driven self-assembly process, resulting in structures that are homogeneous over large lengths (several square centimeters). There should also be a strong input into the field of crystal engineering.³ Solid-state channel structures,^{50,51} related to the fluid columnar cylinder phases reported herein, were found for coordination polymers⁵² and hydrogen-bonding networks.⁵³ Presently, also in the design of crystal

- (41) Smart, B. E. In *Organofluorine Chemistry Principles and Commercial Applications*; Banks, R. E., Smart, B. E., Tatlow, J. C., Eds.; Plenum Press: New York, 1994; pp 57–88.
- (42) (a) Staunton, E.; Christie, A. M.; Andreev, Y. G.; Slawin, A. M. Z.; Bruce, P. G. *Chem. Commun.* **2004**, 148–149. (b) Rhodes, C. P.; Khan, M.; Frech, R. J. *Phys. Chem. B* **2002**, *106*, 10330–10337.
- (43) Due to the confinement by the columns, which penetrate the nematic continuum perpendicular to the nematic director, the director field follows the curvature, and therefore, there is no uniform director in the plane perpendicular to the columns; orientational order is only maintained parallel to the columns. In contrast, there is no disturbance of the nematic director if the columns penetrate the nematic continuum parallel to the long axis of the rods.

- (44) (a) Saez, I. M.; Goodby, J. W.; Richardson, R. M. *Chem. Eur. J.* **2001**, *7*, 2758–2764. (b) Saez, I. M.; Goodby, J. W. *J. Mater. Chem.* **2005**, *15*, 26–40.
- (45) (a) Kishimoto, K.; Yoshio, M.; Mukai, T.; Yoshizawa, M.; Ohno, H.; Kato, T. *J. Am. Chem. Soc.* **2003**, *125*, 3196–3197. (b) Zheng, Y.; Liu, J.; Ungar, G.; Wright, P. V. *Chem. Rec.* **2004**, *4*, 176–191. (c) Judeinstein, P.; Roussel, F. *Adv. Mater.* **2005**, *17*, 723–727.
- (46) (a) Hamley, I. W. *The Physics of Block-Copolymers*; Oxford University Press: Oxford, 1998; pp 24–130. (b) Bates, F. S.; Fredrickson, G. H. *Phys. Today* **1999**, 32–38.
- (47) Morphologies of heteroarm ABC triblock star copolymers: (a) Fujimoto, T.; Zhang, H.; Kazama, T.; Isono, Y.; Hasegawa, H.; Hashimoto, T. *Polymer* **1992**, *33*, 2208–2213. (b) Okamoto, S.; Hasegawa, H.; Hashimoto, T.; Fujimoto, T.; Zhang, H.; Kazama, T.; Takano, A.; Isono, Y. *Polymer* **1997**, *38*, 5275–5281. (c) Sioula, S.; Hadjichristidis, N.; Thomas, E. L. *Macromolecules* **1998**, *31*, 8429–8432. (d) Hückstädt, H.; Göpfert, A.; Abetz, V. *Polymer* **2000**, *41*, 9089. (e) Hückstädt, H.; Göpfert, A.; Abetz, V. *Macromol. Chem. Phys.* **2000**, *201*, 296. (f) Yamauchi, K.; Takahashi, K.; Hasegawa, H.; Iatrou, H.; Hadjichristidis, N.; Kaneko, T.; Nishikawa, Y.; Jinnai, H.; Matsui, T.; Nishioka, H.; Shimizu, M.; Furukawa, H. *Macromolecules* **2003**, *36*, 6962–6966. (g) Jiang, S.; Göpfert, A.; Abetz, V. *Macromol. Rapid Commun.* **2003**, *24*, 932–937. (h) Abetz, V.; Jiang, S.; Göpfert, A. *e-Polym.* **2004**, 040. (i) Abetz, V.; Jiang, S. *e-Polym.* **2004**, 054.
- (48) (a) Watanabe, J.; Sekine, N.; Nematsu, T.; Sone, M.; Kricheldorf, H. R. *Macromolecules* **1996**, *29*, 4816–4818. (b) Thünemann, A. F.; Janietz, S.; Anlauf, S.; Wedel, A. J. *Mater. Chem.* **2000**, *10*, 2652–2656. (c) Fu, K.; Sekine, N.; Sone, M.; Tokita, M.; Watanabe, J. *Polym. J. (Tokyo)* **2002**, *34*, 291–297.
- (49) Prest, P.-J.; Prince, R. B.; Moore, J. S. *J. Am. Chem. Soc.* **1999**, *121*, 5933.
- (50) Examples of supramolecular hexagons, hexagonal cylinders, and hexagonal grids: (a) Venkataraman, D.; Lee, S.; Zhang, J.; Moore, J. S. *Nature* **1994**, *371*, 591–593. (b) Xu, Z.; Lee, S.; Kiang, Y.-H.; Mallik, A. B.; Tsomaia, N.; Mueller, K. T. *Adv. Mater.* **2002**, *13*, 637–641. (c) Lu, J.; Zeng, Q.; Wang, C.; Zheng, Q.; Wan, L.; Bai, C. *J. Mater. Chem.* **2002**, *12*, 2856–2858. (d) Abourahma, H.; Moulton, B.; Kravtsov, V.; Zaworotko, M. J. *J. Am. Chem. Soc.* **2002**, *124*, 9990–9991. (e) Zhao, D.; Moore, J. S. *Chem. Commun.* **2003**, 807–818. (f) Yamamoto, T.; Arif, A. M.; Stang, P. J. *J. Am. Chem. Soc.* **2003**, *125*, 12309–12317. (g) Kim, H.-J.; Zin, W.-C.; Lee, M. J. *J. Am. Chem. Soc.* **2004**, *126*, 7009–7014.

structures, there is an increased thinking in terms of interfaces⁵⁴ and volume fractions of incompatible units.^{2,55} Taking into account multiple-level segregation and including the restrictions given by the rigidity, shape, and molecular topology of some building blocks will contribute to a more sophisticated prediction and design of solid crystal structures. This can lead to a

- (51) Examples of supramolecular squares and square grids: (a) Rakotondradany, F.; Whitehead, M. A.; Lebuis, A.-M.; Sleiman, H. F. *Chem. – Eur. J.* **2003**, *9*, 4771–4780. (b) Dybtsev, D. N.; Chun, H.; Kim, K. *Angew. Chem., Int. Ed.* **2004**, *43*, 5033–5036. (c) Würthner, F.; You, C.-C.; Saha-Möller, C. R. *Chem. Soc. Rev.* **2004**, *33*, 133–146.
- (52) Reviews about coordination polymers: (a) Moulton, B.; Zaworotko, M. J. *Chem. Rev.*, **2001**, *101*, 1629–1658. (b) James, S. L. *Chem. Soc. Rev.* **2003**, *32*, 276–288. (c) Papaefstathiou, G. S.; MacGillivray, L. R. *Coord. Chem. Rev.* **2003**, *246*, 169–184. (d) Zheng, S.-L.; Tong, M.-L.; Chen, X.-M. *Coord. Chem. Rev.* **2003**, *246*, 185–202. (e) Kitagawa, S.; Kitaura, R.; Noro, S. *Angew. Chem., Int. Ed.* **2004**, *43*, 2334–2475.
- (53) (a) Holman, K. T.; Pivovar, A. M.; Swift, J. A.; Ward, M. D. *Acc. Chem. Res.* **2001**, *34*, 107–118. (b) Martin, S. M.; Yonezawa, J.; Horner, M. J.; Macosko, C. W.; Ward, M. D. *Chem. Mater.* **2004**, *16*, 3045–3055. (c) Fournier, J.-H.; Maris, T.; Simard, M.; Wuest, J. D. *Cryst. Growth Des.* **2003**, *3*, 535–540. (d) Bhogala, B. R.; Nangia, A. *Cryst. Growth Des.* **2003**, *3*, 547–554.
- (54) Von Schnering, H. G.; Nesper, R. *Angew. Chem., Int. Ed. Engl.* **1987**, *26*, 1059–1080.
- (55) (a) Xu, Z.; Lee, S.; Lobkovsky, E. B.; Kiang, Y.-H. *J. Am. Chem. Soc.* **2002**, *124*, 123–137. (b) Gordon-Wylie, S. W.; Clark, G. R. *Cryst. Growth Des.* **2003**, *3*, 453–456.

unification of the fields of soft matter engineering (block copolymers and liquid crystals) and crystal engineering. More generally, the systematic investigation of the self-assembly of small but well-designed molecular tectons will undoubtedly contribute to the decoding of the mechanism of molecular information processing during the evolution of complex superstructures, including biological systems.

Acknowledgment. This work was supported by the DFG (GRK 894/1) and the Fonds der Chemischen Industrie. We thank A. Gleeson for help with the synchrotron experiments at SRS Daresbury and CCLRC for the beamtime.

Supporting Information Available: 2D-diffraction pattern of compound **A6/6**, tables with crystallographic data of the mesophases, figure showing the CPK models of compounds **A10/0**–**A10/3**, detailed synthesis schemes, experimental procedures, and analytical data (NMR, MS, and elemental analysis). This material is available free of charge via the Internet at <http://pubs.acs.org>.

JA0535357